BULLETIN OF THE POLISH ACADEMY OF SCIENCES
TECHNICAL SCIENCES, Vol. 73(5), 2025, Article number: e154205
DOI: 10.24425/bpasts.2025.154205



# Flower pollination algorithm optimization applied for Lyapunov-based fuzzy logic speed controller of a complex drive system

**Grzegorz KACZMARCZYK[1], Radosław STANISŁAWSKI[1], Łukasz KNYPIŃSKI[2], Danton Diego FERREIRA[3], and Marcin KAMIŃSKI[1]***

[1] Department of Electrical Machines, Drives and Measurements, Faculty of Electrical Engineering, Wroclaw University of Science and Technology, 50-372 Wroclaw, Poland
[2] Institute of Electrical Engineering and Electronics, Poznan University of Technology, 60-965 Poznan, Poland
[3] Department of Automatic, Federal University of Lavras (UFLA), Minas Gerais, Brazil

**Abstract.** With the current trends in manipulator design, plentiful examples of machines with flexible links and joints can be instantiated. Lighter construction that allows bending and torsion offers multitude of advantages, such as lower energy consumption and better operation safety when collision is possible in the working environment. However, precise control of applications with such mechanical constructions is very challenging. The state variables might be affected by torsional vibrations, and identification of controller parameters is more difficult, which makes the controller tuning complicated. Therefore, this work focuses on tackling the issues related to speed control of electric drives with sophisticated, and elastic couplings. The robustness against parameter uncertainty is provided through the use of a fuzzy logic system. The speed controller design process incorporates the selection of the rule base, designation of membership functions, as well as controller gain optimization using a nature-inspired technique – the flower pollination algorithm (FPA). Increased damping of torsional vibrations, as well as decreased sensitivity to inertia changes is expected compared to other conventional control solutions, such as PI control. In this study both numerical and experimental studies are conducted.

**Keywords:** flower pollination algorithm; fuzzy logic controller; two-mass system electric drives.

## 1. INTRODUCTION

Nowadays, constant growth of quality requirements in many fields of industry can be observed. Huge emphasis is put on the efficiency, versatility, deployment costs and cost-effectiveness of the implemented solutions. The described tendency is also visible in the field of electric drives. As modern technology evolves (including energetic and transport transformation), electric motors are not only used in cooling fans or air conditioners, but they are also an inseparable element of wind turbines [1], electric cars [2], and many other mechanically sophisticated units [3–5]. In order to meet various industrial process demands, electric motors are usually coupled with different load machines. The complexity of modern technological processes often forces the increased sophistication of mechanical part of the machinery. That being said, the complexity of the abovementioned machines often introduces additional disruptions to the system, which impacts the overall control process quality. Moreover, these machines are often coupled with electric motors with the use of long shafts and mechanical clutches, which introduce additional flexibility [6] to the mechanical system. Therefore, the issue of two-mass system control constitutes a huge concern in the field of electric drives automation. In order for the quality of the control system to be approvable, the drive needs to feature excellent dynamics. The overall plant response needs to follow the reference speed/position trajectory accurately, with no visible overshoots or fluctuations. Moreover, in the case of two-mass drive systems, torsional vibrations damping also constitutes an essential issue. Having summed up a variety of two-mass control system requirements it can be stated that bigger complexity of a controlled machine is not a favourable control scenario. The additional elasticity, friction, or even backlash affecting the drive system may lead to serious decrease in effectiveness and accuracy [7, 8]. That being said, it seems justified that the two-mass control system research is still up to date and modern nonlinear control systems are continuously being developed to deal with the occurring inaccuracies [9, 10].

The issue of two-mass drive system control distinguishes several ways to obtain a satisfying plant response. Control theory provides many classical solutions, such as PID (proportional – integral – derivative) controller [11] or state space vector based controller [12]. However, the underlying inconvenience in the mentioned strategies lies in their strict dependency on the plant parameters declared during the tuning process. Thus, the appropriate control strategy featuring increased robustness is a convenient solution in terms of two-mass system control tech-

*e-mail: marcin.kaminski@pwr.edu.pl

Manuscript submitted 2024-09-20, revised 2024-12-26, initially accepted for publication 2025-03-20, published in July 2025.

niques [13]. It provides an eligible plant behaviour in case of significantly changed environment or object parameters, which can fluctuate over time. In order to handle these inconveniences, the utilization of fuzzy logic is a reasonable solution [14]. As a part of robust control techniques, it attenuates the effect of sudden disruptions or time-varying plant parameters.

Fuzzy logic was invented by Lofti Zadeh firstly as a part of mathematics [15], but soon found use in control theory [16]. Its main purpose was to create a convenient tool, which would give scientists the possibility to describe complex, nonlinear phenomena, which are usually hard to represent with mathematical formulas. Using fuzzy logic, the description of the mentioned systems may be easily accomplished with the use of linguistic variables. Due to a wide range of possible applications, fuzzy logic controller constitutes a user-friendly tool, which broadens the robustness and dynamic properties of the controlled systems. A fuzzy logic controller consists of three main layers. The first one is called the fuzzification layer. Its main role is to convert the sharp, numerical values into fuzzified, linguistic variables. After that, proper membership functions are used to calculate the level of particular premiss fulfillment. One of the most important parts of the fuzzy logic controller is the rule base [17], usually described as the second layer of the controller. Its main task is to store a set of pre-defined rules, which describe the dependencies between the controller input and its output. By doing so, after conducting the fuzzification process, it is possible to describe the current state of the plant without the necessity of using a mathematical, state-space equation. Nevertheless, in order to make a fuzzy logic controller work accurately, its design must be performed meticulously. It usually consists of the rule-based definition and the final tuning process. Unfortunately, there are no specific algorithms dedicated to handling the abovementioned implementation difficulties. The last stage includes the defuzzification process, which is responsible for converting the final, linguistic output variable into a numerical one, which is compatible with the further part of the control system. The fuzzy logic controller constitutes an eligible control tool, allowing to obtain satisfying dynamics in terms of complex plants control (i.e., time-varying parameters, e.g., car cruise control system attached to the gearbox). Moreover, it is also a very flexible algorithm, which perfectly cooperates with additional feedbacks (e.g., torsional torque information attached to the fuzzy logic controller). Despite providing necessary features, it is not a convenient solution in terms of deployment easiness. The fuzzy logic controller design and tuning involve using both the designer's experience and optimization (genetic) [18] or other iterative [19] algorithms.

To facilitate the tuning process of the proposed two-mass control system, a nature-inspired algorithm is used. The whole adjustment process is conducted with the use of the flower pollination algorithm (FPA). Its main role is to find the quasi-optimal values of particular controller gains. The whole algorithm is focused on the minimization of the pre-defined cost function. The FPA algorithm is inspired by the pollen distribution process between flowers and plants (local and global optimization). The behaviour of the pollinators is described with the Levy flights [20]. The simplicity of the proposed nature-inspired algorithm (NIA) was one of the main reasons the FPA strategy was chosen [21].

In this article, flower pollination algorithm is used to improve the tuning process of the fuzzy speed controller. The nonlinear fuzzy control strategy is combined with additional torsional torque feedback in order to obtain satisfying plant behaviour. The main point of the research is to verify if the genetic algorithm can be used as a reliable tool, which can make the actual load machine speed follow its reference trajectory more accurately. The paper is organized as follows. The next section includes a brief description of the controlled plant, the main principles of flower pollination algorithm and the overall structure of the proposed control strategy. The third section describes the obtained results of the conducted simulation tests. Then, the fourth stage of the research focuses on the experimental verification of the proposed approach, including a brief description of the used laboratory test bench. The final part of the paper provides the discussion and conclusions of the obtained results.

## 2. DESIGN PROCESS OF THE FUZZY LOGIC SPEED CONTROLLER

### 2.1. Mathematical description of the controlled system

Electric drives with flexible links can be represented as a model consisting of two masses conjoined by an element of finite stiffness. This type of plant is usually referred to as a two-mass system [22]. When transferred to per-unit notation, its mathematical description can be described in the following form:

$$\begin{cases} \dot{\omega}_1 = \dfrac{m_e - m_s}{T_1}, & (1) \\ \dot{\omega}_2 = \dfrac{m_t - m_L}{T_2}, & (2) \\ \dot{m}_t = \dfrac{\omega_1 - \omega_2}{T_c}, & (3) \end{cases}$$

where $\omega_1$, $\omega_2$ are angular speed of the motor and the load machine, $m_e$, $m_t$, $m_L$ are electromagnetic, torsional, and load torques, $T_1$, $T_2$, $T_c$ are mechanical time constants of the motor, the load, and the shaft (respectively). Visual representation of the model is shown in Fig. 1.

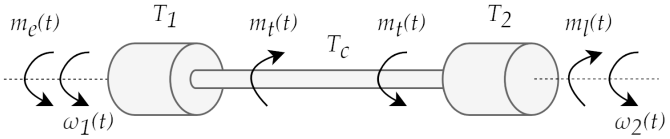


**Fig. 1.** Diagram of a two-mass system

The flexibility of the shaft causes oscillation of the state variables, which is harmful to the controlled drive. Therefore, a controller capable of damping those oscillations needs to be implemented. Usually, detailed knowledge about the plant is needed to determine appropriate values for controller gains [23]. However, there are no direct methods dedicated to fuzzy logic controller tuning. The use of an optimization algorithm needs to be considered to design the controller.

### 2.2. Fundamentals of flower pollination algorithm

Flower pollination algorithm is one of the most common nature-inspired optimization tools. It is based on the flower pollination process which can be observed in nature [21]. In order to obtain a seed or fruit a flower must be pollinated. Usually the whole process concerns the presence of pollinators, but depending on the specific flower/circumstances it is not always mandatory. The pollination can be accomplished within the scope of a single flower or plant. Thus, the above considerations are taken as a base point for the FPA algorithm development. Its general idea distinguishes two types of pollination depending on the area the pollen was transported within. The first variant is called local optimization (abiotic pollination). It describes the case of self-pollination. It refers to the situation where a pollen of a single specimen is transported between the flowers belonging to one plant. The second case of local pollination can be called autogamy. It describes the process of transporting the pollen between the anther and the stigma of an individual flower [24]. Each of the described cases of local pollination does not necessarily require the presence of a pollinator. However, a pollinator (i.e., a bird, a bee, a moth, etc.) is mandatory in order to achieve global pollination, which is also called cross-pollination. It is based on the idea of transporting the pollen between the anther of one flower (plant) to the stigma of another flower (growing on a different plant). The course of the data flow in the FPA algorithm starts with the algorithm initialization (i.e., defining the number of optimized parameters, population size, the cost function equation, switching threshold, and optimized parameters boundaries). Then, in the second step the initial population is drawn. After that, the current population is evaluated with the use of a pre-defined cost function and the best global solution is chosen. A switching parameter value is random in each iteration step. If a random value $\vartheta$ drawn from a normal distribution is below a certain threshold, the global variant is selected. For each flower in the generation, a new value is calculated:

$$\mathbf{x}_i(n+1) = \mathbf{x}_i(n) + L\left(\mathbf{x}_i(n) - \tilde{\mathbf{x}}\right), \tag{4}$$

where $\mathbf{x}_i$ is the currently analyzed flower (solution vector), $\tilde{\mathbf{x}}$ is the currently best solution, $L$ is a number generated from Lévy distribution [20], $n$ is the algorithm iteration counter. The Lévy flight step value is calculated with the use of the following formula:

$$L(n) = \lambda\Gamma(n)\frac{\sin(\frac{\pi\lambda}{2})}{\pi S^{1+\lambda}}, \tag{5}$$

where $S$ is a random step size from the Lévy distribution.

Otherwise, when $\vartheta$ is above the threshold, local pollination is simulated. The future generation is calculated using the following formula:

$$\mathbf{x}_i(n+1) = \mathbf{x}_i(n) + \epsilon\left(\mathbf{x}_j(n) - \mathbf{x}_k(n)\right), \tag{6}$$

where $\mathbf{x}_j$ and $\mathbf{x}_k$ represent pollen of different flowers of the same species as the considered $\mathbf{x}_i$, $\epsilon$ is a random number ($0 \le \epsilon \le 1$).

When pollination is performed on all the flowers in the generation, the value of the cost function $f(\mathbf{x})$ is verified, and if the new solution provides better results, the old one is replaced. The process is repeated for a predefined number of generations of flowers, or until a desired value of the cost function is reached. The overall flowchart of the flower pollination algorithm is presented in Fig. 2.

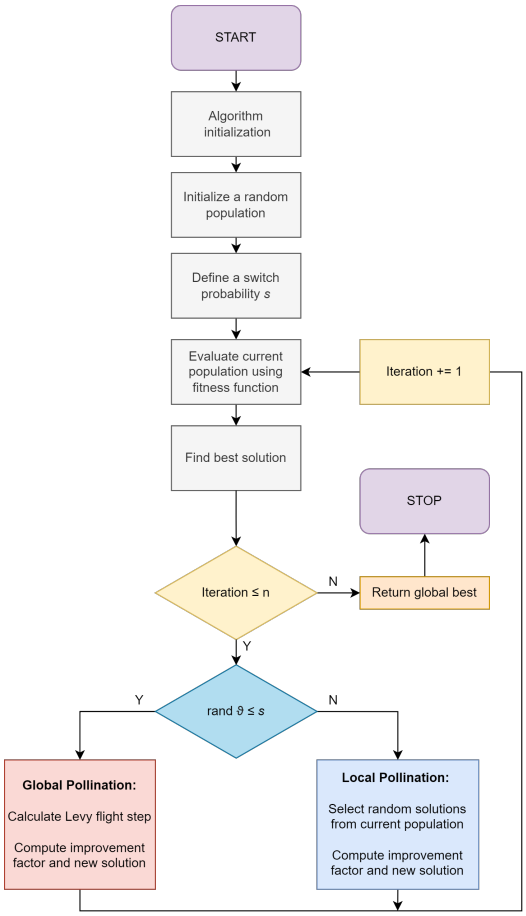


**Fig. 2.** Flowchart of the flower pollination algorithm

### 2.3. Fuzzy logic controller design

The constant growth of dynamic requirements pushes the scientists and engineers to use unconventional tools. Mechanical structure sophistication makes the driven machine appear as a highly nonlinear unit from the point of view of the control system. That being said, it forces modern control structures to be more complex as well. Although, in terms of nonlinear controllers, stability issue is a huge concern as well. Considering the fact, that the design process of the rule base is not a convenient process, a Lyapunov approach is a common one [25].

The rule-base definition begins with a speed error description:

$$e = \omega_{\text{ref}} - \omega_1, \tag{7}$$

$$\dot{e} = -\frac{\mathrm{d}\omega_1}{\mathrm{d}t} = -\dot{\omega}_1. \tag{8}$$

For the stability analysis, the Lyapunov candidate function is chosen:

$$V = \frac{1}{2}\left(q_1^2 + q_2^2\right), \tag{9}$$

where $q_1 = e$, $q_2 = \dfrac{\mathrm{d}e}{\mathrm{d}t} = \dot{e}$. For the system to be stable, the following condition needs to be fulfilled:

$$\dot{V} \leq 0. \tag{10}$$

which can be rewritten as:

$$\dot{V} = q_1\dot{q}_1 + q_2\dot{q}_2 = e\dot{e} + \dot{e}\ddot{e} = \dot{e}(e + \ddot{e}), \tag{11}$$

which, after further transformation can be presented with the following formula:

$$\dot{V} = -\dot{\omega}_1 \left(e + (-\ddot{\omega}_1)\right), \tag{12}$$

Thus, the condition described with equation (10) can also be represented with the following formula:

$$\dot{V} = \dot{\omega}_1 \left(\ddot{\omega}_1 - e\right) \leq 0. \tag{13}$$

Assuming that the derivative of the motor speed is greater than or equal to 0, then the above condition is fulfilled if the following criteria is ensured:

$$\ddot{\omega}_1 - e \leq 0, \tag{14}$$

which can be rewritten as:

$$\ddot{\omega}_1 \leq e. \tag{15}$$

Considering the fact, that:

$$\ddot{\omega}_1 = \frac{d}{dt}\left[\frac{m_e - m_t}{T_c}\right], \tag{16}$$

and assuming, that the derivative of the electromagnetic torque can equate to the control signal, the above equation can be presented in its final form:

$$\frac{1}{T_c}\frac{du}{dt} \leq 0. \tag{17}$$

Having taken the overall controller scheme (presented in Fig. 3) into consideration, the final form of the stability condition can be described with the following formula:

$$\frac{1}{T_c}\frac{d(u_0 - m_t)}{dt} \leq 0. \tag{18}$$

As a consequence of the above equation, in order to make the system stable, the dynamics of the electromagnetic torque (i.e., the control signal) must be higher than the actual dynamics of the torsional torque, which is ensured.

The overall structure of the fuzzy controller is presented in Fig. 3. In this paper, a Takagi-Sugeno model (TSK) was used, due to its simplified microprocessor implementation [17]. In the first stage of the fuzzy controller, the input signals are fuzzified. This operation is mandatory, as it is necessary to describe its value in the form of linguistic variables. The rule base (Table 1) constitutes a critical part of the fuzzy logic controller.

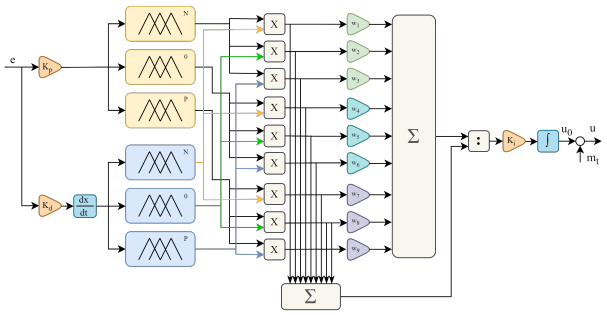

**Fig. 3.** Fuzzy logic speed controller – internal structure

**Table 1**
Rule-base definition

| $e$ | $\dot{e}$ | $u$ |
|---|---|---|
| Negative | Negative | Positive |
| Zero | Negative | Negative |
| Positive | Negative | Zero |
| Negative | Zero | Negative |
| Zero | Zero | Zero |
| Positive | Zero | Positive |
| Negative | Positive | Zero |
| Zero | Positive | Positive |
| Positive | Positive | Negative |

The fuzzified input signals are passed through particular membership functions. As the significance level of each premise is calculated, final rules are attached to each of them. After that, the final control signal is calculated in the process called defuzzification. Its main purpose is to convert the final, linguistic form of the control signal into a crisp variable, which can be transferred to the further part of the control system. In this paper, it is achieved with the use of the singleton method, which can be presented with the following formula:

$$u_0 = \frac{\sum_{i=1}^{n} x_i \cdot w_i}{\sum_{i=1}^{n} x_i} = \frac{\sum_{i=1}^{n} (e \cdot f_1 \cdot \dot{e} \cdot f_2) \cdot w_i}{\sum_{i=1}^{n} x_i}, \tag{19}$$

where $e$, $\dot{e}$ are input signals (error and its time derivative), $f_1$, $f_2$ are membership functions, $w_i$ are weight coefficients (conclusions).

The final form of the control signal (the output of the fuzzy speed controller) includes the actual torsional torque feedback:

$$u = u_0 - m_t\,. \tag{20}$$

### 2.4. The FPA-based tuning of the fuzzy speed controller

In order to present the FPA algorithm as an efficient and feasible tool, basic calculations are conducted, and the parameters of the external loop applied in structure of electric drive with an elastic

connection are selected. Fuzzy logic controller gains (i.e., $K_p$, $K_d$, $K_i$) were chosen as the optimized parameters. As a way to ensure the correctness of the algorithm execution, the following cost function is defined:

$$F_c = \sum(\omega_{\text{ref}} - \omega_1)^2. \tag{21}$$

During the optimization process, the consecutive FPA parameters are assumed:

- $n = 20$ – population size,
- $p = 0.8$ – the probability of switch between local and global pollination,
- $N = 100$ – number of iterations.

The salience of properly performed tuning process is proved by testing the influence of particular gains on the obtained results. The plant response regarding inaccurately adjusted gains is presented in Figs. 4–6. The conditions of the tests are described in the next section. Here, selected parts of the transients presenting the precision of speed control under incorrect values of the investigated coefficients are shown. The main purpose of these tests is to prove the importance of the correct values selection of the speed controller coefficients.

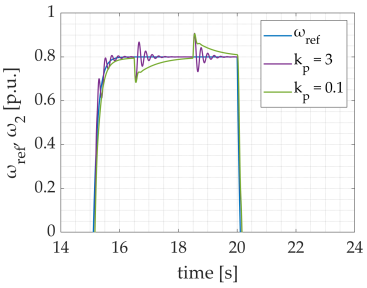


**Fig. 4.** The load speed transients in case of inappropriately selected parameter of the fuzzy controller – the proportional gain

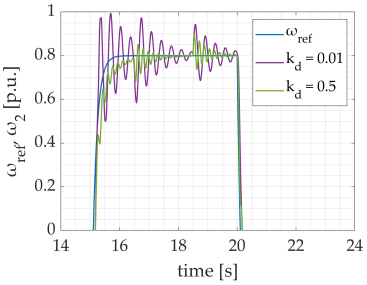


**Fig. 5.** The load speed transients in case of inappropriately selected parameter of the fuzzy controller – the derivative gain

The optimized controller response is described in the following section. The final gain values obtained with the FPA take consecutive values:

- $K_{pFPA} = 0.9172$,
- $K_{dFPA} = 0.075$,
- $K_{iFPA} = 502.88$.

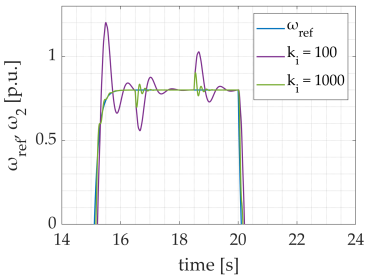


**Fig. 6.** The load speed transients in case of inappropriately selected parameter of the fuzzy controller – the integrator gain

## 3. SIMULATION TESTS

### 3.1. Initial parameters of the simulation model

The simulation tests constitute the first stage of the proposed algorithm verification. In the beginning, it is crucial to create a proper mathematical model of the examined drive system. It is built with the use of transfer function blocks. Each of the consecutive blocks is described with its own time constant, related to the mechanical parameters of the used motors. The used time constants take the following values:

- $T_1 = 0.203$ s,
- $T_c = 0.0026$ s,
- $T_2 = 0.285$ s.

The current control loop represents a current regulator, current measurement unit, and electromagnetic part of the motor with DC-DC (H-bridge) converter. For the sake of simulation research purposes, it can be modelled with the 1-st order inertial block, which can be represented with the following equation:

$$G_e(p) = \frac{1}{T_e(p) + 1}, \tag{22}$$

where $p$ is the Laplace operator, $T_e = 0.0005$ s is the electromagnetic time constant.

Every single electric motor can be described with a specific inertia value, which defines its dynamic properties. As a consequence, it is not capable of following a typical, steep slope square wave. That is the reason why it seems crucial to shape the speed reference signal in a way that can be followed accurately by the motor. The control system with no reference speed filter would not be able to compensate the speed error occurred in the dynamic states of the drive. The applied reference speed trajectory filter used in both simulation and experimental tests can be described with the equation:

$$G_f(p) = \frac{\omega_f^2}{p^2 + 2\zeta\omega_f p + \omega_f^2}, \tag{23}$$

where $\omega_f$ is the angular frequency, $\zeta$ is the damping coefficient. The reference speed trajectory was accomplished by a square wave signal with the consecutive parameters:

- $Amp = 0.8$,
- $f = 0.1$ Hz.

In order to verify the plant behaviour in a variety of different circumstances, the additional load torque is applied to the system

at $t_{s1} = 16.5$ s, and detached at $t_{s2} = 18.5$ s. Its value is equal to the nominal motor torque value. Moreover, to simulate the whole drive power system accurately, the signal constraint is applied to the controller output and equaled to $m_e = 3m_{eN}$. The numerical step length applied to the simulation is set to $T_{\text{step}} = 0.1$ ms.

### 3.2. Preliminary simulation studies

The proposed (optimized) fuzzy logic controller is first applied to numerical tests. The analysis is performed in MATLAB/Simulink environment. All the model components are created with standard library blocks (fuzzy logic toolbox was not used). This way, full access to controller signals is achieved. The presented results are obtained with 0.1 ms numerical step (frequency of calculations). In order to verify the overall plant response in various states (including reversion of the motor speed) of the drive, a square wave is chosen as the form of the reference signal. The achieved simulation results are presented in Figs. 7 and 8.

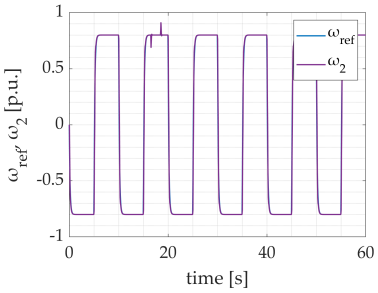


**Fig. 7.** The load speed transient $\omega_2$ in the system with fuzzy controller applied for electric drive with elastic connection

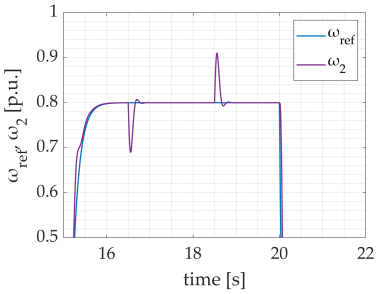


**Fig. 8.** The load speed transient $\omega_2$ in the system with fuzzy controller applied for electric drive with elastic connection – a zoom-in showing the moment of additional load torque attachment ($t = 16.5$ s) and detachment ($t = 18.5$ s)

Analyzing the results obtained during numerical tests several features must be noted. The speed transients presented in Fig. 7 demonstrate the correctness of the plant response. High dynamics of the drive can be noted. The actual load machine speed follows its reference trajectory. A zoom-in to a steady state transition (Fig. 8) shows that a minor lurch is visible just before reaching the steady state. However, the significance of this inconvenience is negligible. Also, significantly mitigated speed transients are achieved under load torque activation. The speed, during the load torque activation, quickly returns to the steady state without causing an overshoot. The same can be said about the moment of load torque deactivation. This is extremely important because those types of dynamic states can deteriorate the durability of the mechanical part of the drive.

In order to examine the designed controller, an additional test is carried out. In the final attempt the impact of the doubled load machine mechanical time constant on the system behaviour is examined. For the purpose of keeping high reliability of the conducted tests, the obtained results are compared with the PI controller behaviour, applied for the same plant. The presented results are shown in Fig. 9. More accurate transients are obtained after using the fuzzy controller. Oscillations are significantly reduced.

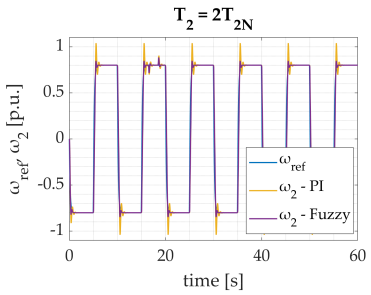


**Fig. 9.** The comparison of the PI and fuzzy logic controllers applied for a two-mass system – increased mechanical time constant

One of the most essential parameters affecting the optimization process is related to the switching coefficient choice. It defines the threshold value, allowing the algorithm to switch between local and global optimization. In order to verify the way its level influences the final plant response an additional test was conducted. It consisted of three examined $s$ coefficient values: $s = 0.5$, $s = 0.8$, and $s = 0.99$. The results of the evaluation are presented in Figs. 10 and 11.

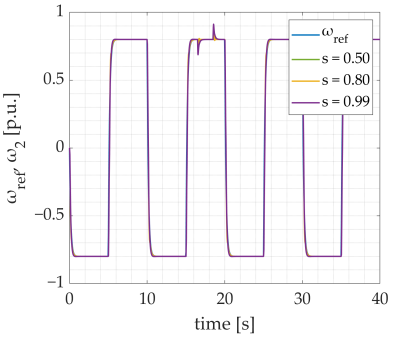


**Fig. 10.** The comparison of the plant response with regard to a different switching coefficient $s$ value defined during optimization process

Having observed the differences between particular numerical attempts it is noticeable that the switching coefficient value has a significant impact on the globally best solution returned by the optimization algorithm. The overall speed transients visible in Fig. 10 do not distinguish salient differences in plant response.

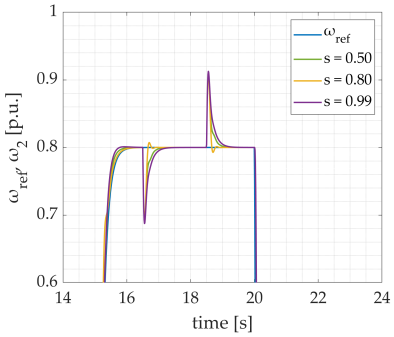


**Fig. 11.** The comparison of the plant response with regard to a different switching coefficient $s$ value defined during optimization process – a zoom-in showing the moment of steady-state transition and additional load torque attachment and detachment

However, a thorough survey of the speed transients presented in Fig. 11 confirms the impact of the switching coefficient on the obtained optimization results. Switching parameter set to $s = 0.5$ provides an eligible plant response. The obtained speed transients feature smooth steady-state transitions and no overshoots. Higher switching parameter provides a plant response featuring better dynamics. However, in the case of $s = 0.8$ additional overshoots occur, which is not a convenient phenomenon. The highest $s$ coefficient value provides the lowest plant response dynamics. Conducted numerical tests confirm the necessity of proper switching coefficient adjustment as it notably affects the results of the optimization process.

## 4. EXPERIMENTAL VERIFICATION

To finalize the research, experimental verification of the numerical results is performed. Experimental tests are carried out on a laboratory stand equipped with a dSPACE DS1103 fast-prototyping device, a 0.5 kW DC motor, and a 0.4 kW DC generator connected to the motor by a long, elastic shaft. The overall scheme of the laboratory test bench is presented in Fig. 12. The whole experimental verification was driven from a PC with ControlDesk software. Analogously to the numerical tests, a square wave is chosen as a reference signal to examine the actual plant behaviour in different states of the drive. The specific parameters of the square signal take consecutive values:

- $f = 0.2Hz$,
- $Amp = 0.4$.

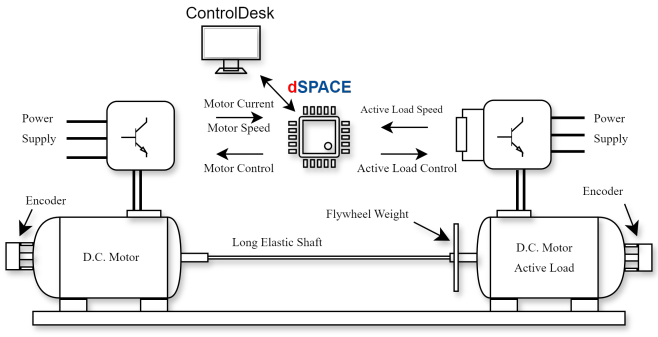


**Fig. 12.** The overall scheme of the laboratory test bench

To make the tests even more reliable, additional load torque is attached to the system every second speed return. A series of the results obtained during the experimental verification is presented in Figs. 13–15.

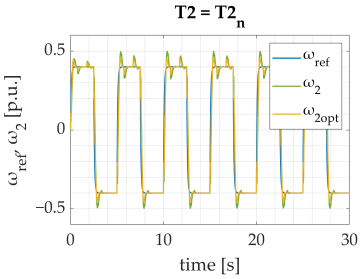


**Fig. 13.** The load speed transient $\omega_2$ in the system with fuzzy controller applied for electric drive with elastic connection – the experimental tests

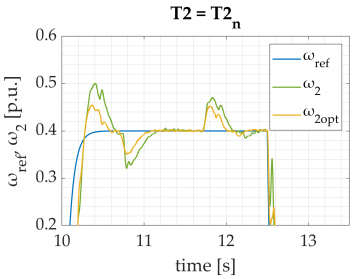


**Fig. 14.** The load speed $\omega_2$ under load torque switching – the experimental tests

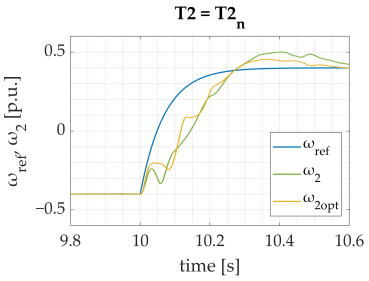


**Fig. 15.** Drive response to change of the speed direction (from counterclockwise to clockwise rotation) – experimental tests

Experimental verification clearly confirms the positive influence of the nature-inspired algorithm on the tuning process. The results presented in Fig. 13 show that the overall system behaviour is eligible. The load machine speed follows its reference trajectory accurately. The zoom-in showing load torque attachment (Fig. 14) confirms appropriate controller gain selection. The structure optimized with the use of FPA features small divergence from the reference value when the additional load torque both appears and disappears. The lurch occurring during load activation is rapidly mitigated, which proves the salience of the optimal tuning process. In addition, the speed transient presented in Fig. 15 confirms the positive influence of the properly tuned controller gains on the load machine speed during steady-state transitions.

In each of the attempts, the presented approach allows to obtain a satisfying plant response. What is more, the control system reaction to sudden load torque occurrence confirms the high reliability of the applied control strategy. Speed error is immediately compensated by the controller. The presented plant behaviour compliments proper system maintenance, as the mechanical part of the drive is not exposed to unpredictable, rapid wrenches. The conducted series of experimental tests proves that the use of NIA is a feasible, user-friendly tool, which gives scientists and engineers a possibility to simplify the tuning process, which also facilitates the overall deployment efficiency.

## 5. FINAL REMARKS

In this paper, an FPA-optimized fuzzy speed controller with additional torsional torque feedback is investigated for possible use with electric drives with an elastic connection. The main contribution of the paper lies in the experimental proof that FPA is a proper tool for selecting fuzzy controller gains. The following advantages were achieved:

- The response of the load speed with the optimized controller values is characterized by no overshoot even though no information about the load speed was provided. Therefore, the reliability of the drive is improved (no load speed sensor is needed).
- Efficient damping of the state variables oscillations is observed.
- After optimization, the drive system handles sudden changes in load torque better – the drop/rise of speed when the active load is applied/disconnected is closer to the desired response.
- A fuzzy-logic-based controller with torsional torque feedback can be easily implemented in numerous programmable devices. The algorithm is not computationally heavy, therefore it would be suitable for many applications.

As mentioned before, there are virtually no direct methods for fuzzy controller tuning. The article proposes a quasi-optimal method for finding appropriate values for the controller gains.

## REFERENCES

[1] Z. Zhang and X. Zhao, "Control of hvdc-connected pmsg-based wind turbines for power system oscillation damping," in *2022 IEEE 13th International Symposium on Power Electronics for Distributed Generation Systems (PEDG)*, 2022, pp. 1–6, doi: 10.1109/PEDG54999.2022.9923123.

[2] S. Zhao, A. Lasson, O. Wallmark, and M. Leksell, "Off-vehicle evaluation of active oscillation damping schemes," *IEEE J. Emerg. Sel. Top. Power Electron.*, vol. 2, no. 2, pp. 264–271, 2014, doi: 10.1109/JESTPE.2013.2291962.

[3] A. Shawky, D. Zydek, Y. Z. Elhalwagy, and A. Ordys, "Modeling and nonlinear control of a flexible-link manipulator," *Appl. Math. Modell.*, vol. 37, no. 23, pp. 9591–9602, 2013, doi: 10.1016/j.apm.2013.05.003.

[4] Q. Meng *et al.*, "Flexible lower limb exoskeleton systems: A review," *NeuroRehabilitation*, vol. 50, no. 4, pp. 367–390, 2022, doi: 10.3233/NRE-210300.

[5] R. Chuei and Z. Cao, "Extreme learning machine-based supertwisting repetitive control for aperiodic disturbance, parameter uncertainty, friction, and backlash compensations of a brushless dc servo motor," *Neural Comput. Appl.*, vol. 32, pp. 14 483–14 495, 2020, doi: 10.1007/s00521-020-04965-w.

[6] L. Zouari, H. Abid, and M. Abid, "Sliding mode and pi controllers for uncertain flexible joint manipulator," *Int. J. Autom. Comput.*, vol. 12, no. 2, pp. 117–124, 2015, doi: 10.1007/s11633-015-0878-x.

[7] X. Dong, K. Shi, and W. Li, "Residuanourlurll vibration control of a single-link flexible manipulator with variable stiffness and damping magnetorheological joint," *J. Phys.-Conf. Ser.*, vol. 1678, no. 1, p. 012005, Nov 2020.

[8] J. Padron, Y. Kawai, Y. Yokokura, K. Ohishi, and T. Miyazaki, "Stable torsion torque control based on friction-backlash analogy for two-inertia systems with backlash," *IEEJ J. Ind. Appl.*, vol. 11, no. 2, pp. 279–290, 2022, doi: 10.1541/ieejjia.21004543.

[9] W. Alam, A. Mehmood, K. Ali, U. Javaid, S. Alharbi, and J. Iqbal, "Nonlinear control of a flexible joint robotic manipulator with experimental validation," *Strojniski Vestnik*, vol. 64, 01 2018.

[10] M. Sayahkarajy, Z. Mohamed, and A.A. Mohd Faudzi, "Review of modelling and control of flexible-link manipulators," *Proc. Inst. Mech. Eng. Part I-J Syst Control Eng.*, vol. 230, no. 8, pp. 861–873, 2016, doi: 10.1177/0959651816642099.

[11] C. Mendil, M. Kidouche, and M.Z. Doghmane, "Hybrid sliding pid controller for torsional vibrations mitigation in rotary drilling systems," *Indones. J. Electr. Eng. Comput. Sci.*, vol. 22, no. 1, pp. 146–158, 2021, doi: 10.11591/ijeecs.v22.i1.pp146-158.

[12] M. Malarczyk, M. Zychlewicz, R. Stanislawski, and M. Kaminski, "Speed control based on state vector applied for electrical drive with elastic connection," *Automation*, vol. 3, no. 3, pp. 337–363, 2022.

[13] G. Kaczmarczyk, R. Stanislawski, M. Kaminski, K. Kasprzak, and D.D. Ferreira, "A neural-enhanced active disturbance load-side speed control of an electric drive with a flexible link," *Arch. Electr. Eng.*, vol. vol. 74, p. 269–289, 2025, doi: 10.24425/aee.2025.153024.

[14] M.E. Akbari, M.A. Badamchizadeh, and M.A. Poor, "Implementation of a fuzzy tsk controller for a flexible joint robot," *Discrete Dyn. Nat. Soc.*, vol. 2012, no. 1, p. 279498, 2012.

[15] L. Zadeh, "Fuzzy sets," *Inf. Control*, vol. 8, no. 3, pp. 338–353, 1965, doi: 10.1016/S0019-9958(65)90241-X.

[16] L.A. Zadeh, "A rationale for fuzzy control," *J. Dyn. Syst. Meas. Control*, vol. 94, no. 1, pp. 3–4, 03 1972, doi: 10.1115/1.3426540.

[17] G. Kaczmarczyk, M. Malarczyk, D.D. Ferreira, and M. Kaminski, "Stable rules definition for fuzzy ts speed controller implemented for bldc motor," *Appl. Sci.*, vol. 14, no. 3, 2024, doi: 10.3390/app14030982.

[18] M.S. Abou Omar, T.Y. Khedr, and B.A. Abou Zalam, "Particle swarm optimization of fuzzy supervisory controller for nonlinear position control system," in *2013 8th International Conference on Computer Engineering Systems (ICCES)*, 2013, pp. 138–145, doi: 10.1109/ICCES.2013.6707189.

[19] A. Sakalli, T. Kumbasar, and J.M. Mendel, "Towards systematic design of general type-2 fuzzy logic controllers: analysis, interpretation, and tuning," *IEEE Trans. Fuzzy Syst.*, vol. 29, no. 2, pp. 226–239, 2020, doi: 10.1109/TFUZZ.2020.3016034.

[20] A. Chechkin, R. Metzler, J. Klafter, and V. Gonchar, *Introduction to the Theory of Lévy Flights*. Wiley, 09 2008, pp. 129–162, doi: 10.1002/9783527622979.ch5.

[21] X.-S. Yang, "Flower pollination algorithm for global optimization," in *Unconventional Computation and Natural Computation*, J. Durand-Lose and N. Jonoska, Eds. Berlin, Heidelberg: Springer Berlin Heidelberg, 2012, pp. 240–249, doi: 10.1007/978-3-642-32894-7_27.

[22] G. Kaczmarczyk, R. Stanislawski, J. Szrek, and M. Kaminski, "Adaptive sliding mode control based on a radial neural model applied for an electric drive with an elastic shaft," *Energies*, vol. 17, no. 4, 2024, doi: 10.3390/en17040833.

[23] K. Szabat and T. Orlowska-Kowalska, "Vibration suppression in a two-mass drive system using pi speed controller and additional feedbacks—comparative study," *IEEE Trans. Ind. Electron.*, vol. 54, no. 2, pp. 1193–1206, 2007, doi: 10.1109/TIE.2007.892608.

[24] M. Malarczyk, G. Kaczmarczyk, J. Szrek, and M. Kaminski, "Internet of robotic things (iort) and metaheuristic optimization techniques applied for wheel-legged robot," *Future Internet*, vol. 15, no. 9, 2023, doi: 10.3390/fi15090303.

[25] R.-E. Precup, M. Tomescu, and S. Preitl, "Fuzzy logic control system stability analysis based on lyapunov's direct method," *Int. J. Comput. Commun. Control*, vol. 4, pp. 415–426, 12 2009, doi: 10.15837/ijccc.2009.4.2457.